Journal Pre-proof

Molecular Imaging of the Serotonin Transporter Availability and Occupancy by Antidepressant Treatment in Late-Life Depression

Gwenn S. Smith, Hiroto Kuwabara, Neda F. Gould, Najilla Nassery, Alena Savonenko, Jin Hui Joo, Kristin Bigos, Michael Kraut, James Brasic, Daniel P. Holt, Andrew W. Hall, William B. Mathews, Robert F. Dannals, Ayon Nandi, Clifford I. Workman
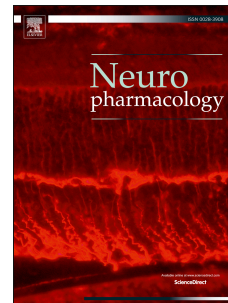
Please cite this article as: Smith, G.S., Kuwabara, H., Gould, N.F., Nassery, N., Savonenko, A., Joo, J.H., Bigos, K., Kraut, M., Brasic, J., Holt, D.P., Hall, A.W., Mathews, W.B., Dannals, R.F., Nandi, A., Workman, C.I., Molecular Imaging of the Serotonin Transporter Availability and Occupancy by Antidepressant Treatment in Late-Life Depression, *Neuropharmacology*, https://doi.org/10.1016/j.neuropharm.2021.108447.

This is a PDF file of an article that has undergone enhancements after acceptance, such as the addition of a cover page and metadata, and formatting for readability, but it is not yet the definitive version of record. This version will undergo additional copyediting, typesetting and review before it is published in its final form, but we are providing this version to give early visibility of the article. Please note that, during the production process, errors may be discovered which could affect the content, and all legal disclaimers that apply to the journal pertain.

The Credit Author Statement is as follows:

Smith: Conceptualization, Methodology, Validation, Formal Analysis, Investigation, Data curation, Writing (original draft), Writing (Review and Editing), Project Administration, Funding acquisition

Kuwabara: Methodology, Validation, Formal analysis, Visualization, Writing (original draft), Writing (Review and Editing)

Gould: Investigation, Writing (original draft), Writing (Review and Editing)

Nassery: Investigation, Writing (original draft), Writing (Review and Editing)

Savonenko: Writing (original draft), Writing (Review and Editing)

Joo: Investigation

Bigos: Writing (original draft), Writing (Review and Editing)

Kraut: Investigation, Writing (original draft), Writing (Review and Editing)

Brasic: Investigation, Writing (original draft), Writing (Review and Editing)

Holt: Investigation

Hall: Investigation

Matthews: Investigation

Dannals: Investigation

Nandi: Methodology, Validation, Formal Analysis, Investigation, Data curation

Workman: Conceptualization, Methodology, Validation, Formal Analysis, Investigation, Data curation, Writing (original draft), Writing (Review and Editing), Project Administration, Funding acquisition

Molecular Imaging of the Serotonin Transporter Availability and Occupancy by Antidepressant Treatment in Late-Life Depression

Gwenn S. Smith, PhD[1,2]*, Hiroto Kuwabara, MD, PhD[2], Neda F. Gould, PhD[1], Najilla Nassery, MD, MPH[4], Alena Savonenko, MD, PhD[5], Jin Hui Joo, MD[1,] Kristin Bigos, PhD[1,6], Michael Kraut, MD, PhD[3], James Brasic, MD[2], Daniel P. Holt, MS[2], Andrew W. Hall, MS[2], William B. Mathews[2], PhD., Robert F. Dannals, PhD[2], Ayon Nandi, BS[2], Clifford I. Workman, PhD[1]

[1]Department of Psychiatry and Behavioral Sciences, Johns Hopkins University School of Medicine, Baltimore, MD
[2]Division of Nuclear Medicine and Molecular Imaging, [3]Division of Neuroradiology, Russell H. Morgan Department of Radiology and Radiological Sciences, Johns Hopkins University School of Medicine, Baltimore, MD
[4]Division of General Internal Medicine, Department of Medicine, Johns Hopkins University School of Medicine, Baltimore, MD
[5]Department of Pathology (Neuropathology), Johns Hopkins University School of Medicine, Baltimore, MD
[6]Department of Medicine (Clinical Pharmacology) and Pharmacology and Molecular Sciences, Johns Hopkins University School of Medicine, Baltimore, MD

Please address all correspondence and reprint requests to:
Gwenn S. Smith, Ph.D.
Richman Family Professor
Department of Psychiatry and Behavioral Sciences
Division of Geriatric Psychiatry and Neuropsychiatry
Johns Hopkins University School of Medicine
Johns Hopkins Bayview Medical Center
5300 Alpha Commons Drive, 4th floor
Baltimore, MD 21224
Phone: 410-550-6207
Fax: 410-550-1407
Email address: gsmith95@jhmi.edu

Running Title: Serotonin Transporter in Late-Life Depression

Key words: selective serotonin reuptake inhibitors, Citalopram, Sertraline, serotonin transporter, positron emission tomography (PET), late-life depression, aging

1

2

ABSTRACT

Patients with late-life depression (LLD) have a more variable response to antidepressant treatment relative to patients with mid-life depression. The neurobiological mechanisms underlying the variability in treatment response are not well understood and may involve the serotonin system. The focus of this study was to test the hypotheses that lower cortical and limbic serotonin transporter (5-HTT) availability in LLD patients relative to controls and less 5-HTT occupancy with antidepressant medications would be associated with less improvement in mood and cognition with treatment in LLD patients. Twenty LLD patients meeting DSM-IV criteria for a current major depressive episode and 20 non-depressed controls underwent clinical and neuropsychological assessments, magnetic resonance imaging to measure grey matter volumes and high-resolution positron emission tomography (PET) scanning to measure 5-HTT before and after 10-12 weeks of treatment with Citalopram or Sertraline (patients only). Prior to treatment, 5-HTT was lower in LLD patients relative to controls in temporal cortical and limbic (amygdala) regions. Grey matter volumes were not significantly different between groups. 5-HTT occupancy was detected throughout cortical, striatal, thalamic and limbic (amygdala, hippocampus) regions. The magnitude of regional 5-HTT occupancy by antidepressants was 70% or higher, consistent with or greater than the magnitude of 5-HTT occupancy observed in mid-life depressed patients. Greater regional 5-HTT occupancy correlated with greater improvement in depressive symptoms and visual-spatial memory performance. These data support the hypothesis that serotonin degeneration and variability in 5-HTT occupancy may contribute to heterogeneity in mood and cognitive responses to antidepressant treatment in LLD patients.

3

1.0 INTRODUCTION

Depression in late life is associated with disability, greater mortality and increased risk of all-cause dementia, including Alzheimer's (AD) and vascular dementia (Alexopoulos et al., 1996; Bruce and Leaf, 1989; Diniz et al., 2013). While there are effective antidepressant agents these treatments have been developed for the treatment of depression in younger patients. More than half of depressed older adults patients have partial response to medication or are treatment refractory (Dew et al., 1997). Even after remission of their depressive symptoms, many older adults have persistent cognitive impairment (in executive function, memory and motor speed; Alexopoulos et al., 1993; Bhalla et al., 2006). The neurobiological mechanisms underlying variable treatment response of mood symptoms and cognitive deficits in late-life depression (LLD) has not been a major focus of investigation. For example, decreased gray matter volumes have not been reported consistently in LLD patients relative to controls (especially in patients who do not have substantial cognitive deficits) and have not been associated consistently with treatment response (Jamieson et al., 2019). Several lines of evidence support the study of the serotonin system as a logical focus. The serotonin system has been implicated in the neurobiology of depression and is a primary target for the most commonly used antidepressants, selective serotonin reuptake inhibitors (SSRI's; (Coppen, 1967; Schildkraut, 1965). There is considerable evidence for the vulnerability of the serotonin system in aging and neurodegenerative diseases, as well as for its role in both neuropsychiatric symptoms and cognitive deficits (Trillo et al., 2013). The widespread serotonin innervation in cortical and limbic regions overlaps with regions vulnerable to neurodegeneration, as well as to the network changes observed with antidepressant treatment (Varnäs et al., 2004; Diaconescu et al., 2011).

Molecular imaging methods can be applied to understand the neurobiological mechanisms underlying variability in antidepressant treatment response. The serotonin system has been a major focus of radiotracer development for positron emission tomography (PET). Well-validated radiotracers have been developed for the serotonin transporter (5-HTT), as well as for serotonin receptors (including 5-HT1a, 5-HT1b, 5-HT2A, 5-HT4 and 5-HT6 receptors; as reviewed by Kumar and Mann, 2014). These radiotracers have been used to address fundamental questions regarding degeneration of the serotonergic system in aging and in psychiatric and neurodegenerative diseases and its role in SSRIs treatment response (Smith et al., 2017, Lanzenberger et al., 2012; Meyer et al., 2001; Parsey et al., 2006b). A major application of these radiotracers has been to test the serotonin hypothesis of depression (Spies et al., 2015). Most of these studies have been performed in mid-life depressed patients. Initial studies in LLD patients have demonstrated a comparable magnitude and regional localization of 5-HTT occupancy by Citalopram as patients with mid-life depression (Smith et al., 2011). The relationship of 5-HTT antidepressant occupancy by antidepressants to change in depressive symptoms and neuropsychological deficits has been a more limited area of study (Lanzenberger et al., 2012). 5-HTT occupancy may play a more important role in variability in treatment response in older adults with depression,

4

which may be due to such factors as age-related pharmacokinetic changes and degeneration of the serotonergic system.(Boyce et al., 2012; Trillo et al., 2013).

The focus of the present study was to measure 5-HTT availability using PET in LLD patients and compared to demographically matched controls. 5-HTT PET scanning was repeated in the LLD patients during a twelve-week treatment trial with the antidepressants, Citalopram or Sertraline. Correlations were performed between regional 5-HTT availability and occupancy with both depressive symptoms and neuropsychological outcomes. The hypotheses were tested that 1) lower 5-HTT availability will be observed in LLD patients relative to controls in frontal and temporal cortices and limbic regions (amygdala and hippocampus), in contrast to no differences in gray mater volumes, 2) 5-HTT occupancy in frontal, temporal striatal and limbic regions will be observed in LLD patients and 3) lower baseline 5-HTT availability and less 5-HTT occupancy after antidepressant treatment will correlate with less improvement in depressive symptoms and cognition in LLD patients.

2.0 MATERIALS AND METHODS

The LLD patients and healthy controls completed screening assessments and then, magnetic resonance imaging (MRI) and 5-HTT PET scanning, as well as clinical and neuropsychological assessments. The, the LLD patients underwent a twelve-week treatment trial with the antidepressants Citalopram or Sertraline. Clinical and neuropsychological assessments were repeated after 10-12 weeks of treatment, at which time a stable clinical response was achieved. 5-HTT PET scans were repeated to measure 5-HTT occupancy by SSRIs.

2.1 Participant Screening and Selection

Participants were recruited from advertisements in the community or from the Johns Hopkins University Alzheimer's Disease Research Center (2P50AG005146). The screening procedures included a physical and neurological examination, laboratory testing and toxicology screening and psychiatric and neuropsychological evaluations. A Structured Clinical Interview for DSM-IV by a clinical psychologist (NG), the antidepressant treatment history form (Sackeim, 2001)., Clinical Dementia Rating scale (CDR) and a Mini Mental State Examination were administered (MMSE; First et al., 1995; Folstein et al., 1975; Morris, 1993). LLD patients were enrolled who were over age 60 and who had a DSM-IV diagnosis of current major depressive episode (non-bipolar, non-psychotic) and a Hamilton Depression Rating Scale Scores of 17 or higher (HAMD; 24 item scale; Hamilton, 1960). Participants were excluded from enrollment based on the following criteria: 1) had a history of or active neurological or Axis I psychiatric disorders (including dementia), except for a diagnosis of current major depressive episode (non-bipolar, non-psychotic) in the LLD patients; 2) were not medically stable

5

(i.e. poorly controlled medical conditions including hypertension and/or diabetes); 3) a positive toxicology screening or use of psychotropic drugs or medications with central nervous system effects (e.g. antihistamines, cold medications) within two weeks prior to enrollment and 4) contraindications for undergoing MRI scans (e.g. pacemaker, metal implants, aneurism clamps). The study protocol and consent forms were approved by the Institutional Review Board and the Radiation Research Committee of the Johns Hopkins University School of Medicine. Participants received a transcribed and verbal description of the study and written informed consent was obtained.

2.2 Antidepressant Treatment

After the baseline procedures were completed (clinical and neuropsychological assessments, MRI and 5-HTT PET scans), LLD patients were started on a one week course of Citalopram (10 mg once daily). All patients were followed, on a weekly basis. Clinical ratings for depression and anxiety symptoms and side effects were performed (HAMD; Hamilton, 1960) Beck Depression Inventory (BDI; (Beck and Steer, 1993) and the Clinical Global Impression Scale (CGI; Guy, 2008). If the LLD patients did not demonstrate significant clinical improvement defined by a rating of 3 or greater on the CGI, the dose was increased to 20mg per day. If there was no significant improvement on the 20mg dose after 3 weeks, the 20mg dose was increased to 30mg daily and then to 40mg daily for a total of 12 weeks of treatment. During the course of the study, a 'black' box' warning was issued for Citalopram (Vieweg et al., 2012). The study protocol was changed at that time to the use of the SSRI, Sertraline. The last 3 subjects enrolled were treated with Sertraline. LLD patients received 25mg per day for two weeks and subsequently had the dose increased by 25mg each week to a maximum dose of 150mg, if they did not achieve significant clinical improvement (rating of 3 or greater on the CGI) at each dose. The HAMD was performed bi-weekly. Response was determined based on the HAMD ratings from weeks 8 to 12. The criteria for treatment response was a HAMD score of 10 or below for two consecutive weeks (Dew et al., 1997). Plasma Citalopram or Sertraline concentrations were determined every four weeks, including a sample obtained immediately prior to injection of the radiotracer for the second 5-HTT PET scan (Supplemental data; Øyehaug et al., 1982; Suckow et al., 1992).

2.3 Neuropsychological Testing

A multi-domain neuropsychological test battery was administered to the LLD patients and controls at baseline and after 10-12 weeks of pharmacotherapy (patients only), including cognitive domains that are known to be affected in LLD patients and those that are shown to improve with antidepressant treatment (Butters et al., 2004a, 2004b; Lockwood et al., 2002). The Delis-Kaplan Executive Function System Letter and Category Fluency*, Trail Making Test,* Color-Word Interference Test* and Sorting Test* were used to measure executive function (Delis et al., 2006). The California Verbal Learning Test (CVLT)* and Wechsler Memory

Scale*, Logical Memory were used to measure auditory-verbal memory (Delis et al., 1987; Wechsler, 1997). The visual-spatial memory tests used were the Brief Visual Memory Test-Revised (BVMT-R)* and the Rey Complex Figure Test (Benedict, 1997; Rey, 1941). The Symbol Digit Modalities Test was used to measure attention (Smith, 1968). The Iowa Gambling Test was used to measure attention (Bechara, 2007). For repeated testing, alternate forms of the tests were used where available (*).

2.4 MR Imaging Procedures

All participants underwent MRI scanning before the 5-HTT PET scan. MRIs of the brain were acquired at the F. M. Kirby Research Center for Functional Brain Imaging of the Kennedy Krieger Institute. A Phillips 3.0T Achieva MRI instrument was used with an 8-channel head coil (Philips Medical Systems, Best, Netherlands). The magnetization-prepared rapid acquisition with gradient-echo (MPRAGE) pulse sequence (TE = 4, TR = 8.9, flip angle = 8 degrees, NSA = 1, 0.7mm isotropic voxel size) was used for volumetric analyses and MRI to PET co-registration.

2.4 PET Imaging Procedures

PET scans were acquired at the PET Center, Russell H. Morgan Department of Radiology, Johns Hopkins University School of Medicine. The scanner used was a second-generation High Resolution Research Tomograph scanner (HRRT, Siemens Healthcare, Knoxville, TN), a cerium-doped lutetium oxyorthosilicate (Lu25i05[Ce]; LSO) based, dedicated brain PET scanner. Each subject was fitted with a thermoplastic mask modeled to their face to reduce head motion during the PET study. Attenuation maps were generated from a six-minute transmission scan performed with a [^{137}Cs] point source prior to the emission scans.

A well-characterized radiotracer for 5-HTT availability, employed in the majority of previous 5-HTT PET studies was used (Spies et al. 2011). The radiotracer [^{11}C]-3-amino-4-(2-dimethylaminomethyl-phenylsulfanyl)-benzonitrile ([^{11}C]-DASB), synthesized as previously described, was used to measure 5-HTT availability (Wilson et al., 2002). Dynamic scanning began immediately upon a 20 mCi ±10% radiotracer injection and lasted for ninety minutes. The data were acquired in list mode. The images were reconstructed using the iterative ordered subset expectation maximization (OS-EM) algorithm (with 6 iterations and 16 subsets), with correction for radioactive decay, dead time, attenuation, scatter and randoms, (Rahmim et al., 2005) and re-binned into thirty frames (four 15 seconds, four 30 seconds, three 1 minute, two 2 minute, five 4 minute, and twelve 5 minute frames). The reconstructed image space consisted of 256 (left-to-right) by 256 (nasion-to-inion) by 207 (neck-to-cranium) cubic voxels, each 1.22 mm in dimension. The final spatial resolution was less than 2.5 mm full width at half-maximum (FWHM) in three directions (Sossi et al., 2005).

7

2.5 MRI Processing and Analysis

The MPRAGE images were analyzed to delineate volumes of interest (VOIs) on the MRI scans that were copied onto the PET scan, to develop a study specific mask for spatial normalization of the PET images for voxel-wise analyses, and to perform voxel based morphometry (VBM) analyses of between-group differences in grey matter volumes. MRI scans were submitted to Freesurfer (FS v6.0; (Fischl et al., 2002)) for automated parcellation of brain regions that consisted of 82 left and right cortical and subcortical volumes of interest (VOIs) and the whole cerebellum gray matter. The VOIs were transferred from MRI to PET space using PET-to-MRI co-registration parameters that were obtained using the co-registration module in SPM12 (SPM12; Institute of Neurology, London) running on MATLAB 7.10 (MathWorks, Natick, Massachusetts).

FS-derived gray and white matter (GM and WM, respectively) masks of individual subjects were submitted to the "Diffeomorphic Anatomical Registration Through Exponentiated Lie Algebra" (DARTEL) algorithm (Ashburner, 2007) to obtain a pair of GM and WM templates. The templates were spatially registered to the Montreal Neurological Institute (MNI) space and GM and WM masks of individual subjects were spatially normalized to the MNI space in the final step of DARTEL. So-obtained GM and WM masks were averaged across subjects to obtain FS-based GM and WM templates and inserted to SPM-supplied 6 layer templates (i.e., TPM.nii) to be FS-derived 6 layer templates. The FS-derived templates were used for spatial normalization of functional images-subject-specific GM and WM templates in Montreal Neurological Institute (MNI) space. FS-derived GM masks were spatially normalized to so-obtained GM mask using the 'preserved' option and smoothed by a Gaussian kernel of 8 mm FWHM (Ashburner, 2007). VBM was performed to evaluate group differences in grey matter volumes using SPM12.

2.6 PET Tracer Kinetic Modelling and Image Processing

Regional binding potential (BP_{ND}) values of [^{11}C]DASB were obtained using the reference tissue graphical analysis (RTGA; Innis et al., 2007; Logan et al., 1996) The cerebellar grey matter excluding the vermis was used as the reference region. Briefly, the start of the model assumption (t*; the time for the free-plasma ratio approaches time-invariant) was set to 25 minutes. The brain-to-blood clearance rate constant (k2R) of the cerebellum was set to 0.048 min^{-1}, which corresponded to a population mean value of k2R from the multilinear reference tissue method with 2 parameters (MRTM2; Ichise et al., 2003) To reduce noise-dependent underestimation of BP_{ND} seen on BP_{ND} maps from RTGA, BP_{ND} maps were generated by RTGA using dynamic PET frames that were smoothed by a 6mm (FWHM) Gaussian kernel. The VOIs for the cortical lobes were averaged and for right and left hemispheres to yield 44 and the brainstem VOIs (Desikan et al., 2006).
The VOI data were also analyzed by subdividing the VOIs according to the Braak stages of Tau accumulation. (Braak and Braak, 1991; Schöll et al., 2016). The stages were defined as follows: Stage I (Entorhinal cortex),

8

Stage II (Hippocampus), Stage III (Amygdala, Parahippocampus, Fusiform gyrus, Lingual gyrus,), Stage IV (Caudal anterior cingulate, Rostral anterior cingulate, Insula, Temporal pole, Middle temporal lobe, Inferior temporal lobe, Isthmus/cingulate, Posterior cingulate, Thalamus), Stage V (Caudal middle frontal, Rostral middle frontal, Superior frontal lobe, Frontal operculum, Frontal pole, Bank of the superior temporal sulcus, Inferior parietal lobe, Lateral occipital lobe, Lateral orbital gyrus, Medial orbital gyrus, Orbital operculum, Pars triangularis, Superior temporal lobe, Transverse temporal, Precuneus, Superior parietal lobe, Supramarginal gyrus, Caudate nucleus, Putamen, Ventral striatum) and Stage VI (Precentral gyrus, Postcentral gyrus, Paracentral, Pericalcarine gyrus, Cuneus).

Regional 5-HTT occupancy was calculated from the PET VOIs by the following formula: $(BP_{ND}B - BP_{ND}T)/BP_{ND}B \cdot 100$ (%) where $BP_{ND}B$ and $BP_{ND}T$ stand for BP_{ND} values of baseline and post-treatment scans, respectively. Scatter plots of occupancy data versus plasma Citalopram concentrations were fitted to the first order Hill's equation: Occupancy = $O_{max} \cdot$ plasma Citalopram concentrations /(half maximal inhibitory concentration [IC_{50}]+ plasma Citalopram concentrations) where O_{max} stands for the maximal attainable occupancy, and IC_{50} stands for the plasma Citalopram concentrations that causes 50% of O_{max}. The 5-HTT occupancy- plasma Citalopram relationships were examined in regions whose mean BP_{ND} values before treatment were greater than 0.5. The Akaike information criterion (AIC; (Akaike, 1974) was used for the model selection using the following formula: AIC = $2 \cdot k + n \cdot \log(RSS)$ where k, n, and RSS stand for the number of parameters, number of data point and the residual sum of squares, respectively.

The pre-processing of the parametric [^{11}C]-DASB BP_{ND} images was performed with SPM12. First, as mentioned, MRIs were spatially normalized to MNI space using the FS-derived 6-layer template from DARTEL in place of the SPM-supplied template. Second, the paired [^{11}C]-DASB BP_{ND} images for the LLD patients were first co-registered to each other and then, all of the [^{11}C]-DASB BP_{ND} images were transferred to MNI space by combining spatial normalization and PET-to-MRI co-registration parameters. The BP_{ND} images in MNI space were smoothed with a 5mm (FWHM) Gaussian kernel. The combination of smoothing of the dynamic PET frames with smoothing of the BP_{ND} images is equivalent to smoothing the native PET images with an 8mm (FWHM) Gaussian kernel. A binarized FS-derived GM + WM mask, after smoothing with a 10mm (FWHM) Gaussian kernel (height threshold = 0.2) limited the search area (explicit mask).

2.7 Statistical Analyses

One-way and repeated-measures analyses of variance were used to test between and within group differences, respectively, in demographic, clinical and neuropsychological variables and the VOIs for 5-HTT availability (SPSS, version 26). Given the number of neuropsychological measures, the most relevant outcome measure for each test was used in the statistical analysis and a False Discovery Rate significance correction

9

was used (FDR=0.05; $P \geq 0.001$). Exploratory, voxel-wise statistical analyses were performed in SPM12. The two-sample t-test option was used to test for between group differences in 5-HTT availability. The multiple regression option was used to correlate baseline 5-HTT with clinical and neuropsychological variables in the LLD patients and controls. The paired T-test option was used to compare the 5-HTT PET scans before to the scans during SSRI treatment. As the magnitude of 5-HTT occupancy for Citalopram and Sertraline are similar, based on prior [11C]-DASB studies, the data for the two treatment groups were combined (Meyer et al., 2004). For the LLD patients, the multiple regression option was used to correlate the difference between the 5-HTT parametric images before to during treatment with the differences in clinical and neuropsychological variables.

The significance criteria used for reporting the results of the exploratory, voxel-wise analyses for the between-group t-tests and multiple regression results was a cluster-level, family-wise error (FWE)-corrected threshold of $P \leq 0.05$ and a peak voxel uncorrected threshold of $P \leq 0.001$: Height threshold p=0.01 and extent threshold (k) =50 voxels. Given the magnitude of the change in 5-HTT availability with SSRI treatment, results were reported at a more stringent, cluster-level FWE-corrected threshold of $P \leq 0.001$ and a corrected voxel-level threshold of $P \leq 0.001$: Height threshold $P = 0.001$ and extent threshold (k) =50 voxels. The peak voxels within anatomical regions belonging to the same cluster are represented on different rows on each of the tables. Brain locations are reported as x, y, z coordinates in MNI space with approximate Brodmann areas (BA) identified by mathematical transformation into Talairach space with a non-linear mapping approach (Lacadie et al., 2008).

3.0 RESULTS

3.1 Demographic, Clinical and Neuropsychological Measures: Twenty LLD patients and 20 healthy controls were enrolled. Nineteen patients completed the follow-up cognitive and neuroimaging procedures. 522 patients were screened by telephone and 34 in person (14 were screening failures). The reasons for not meeting eligibility criteria included 38% for current psychotropic drug use, psychiatric co-morbidities or claustrophobia, 43% for not being medically stable or having other medical exclusionary criteria and 18% who were not interested in medication or neuroimaging or did not have an informant). The demographic characteristics, clinical and neuropsychological results are shown in Table 1. Only one patient had been treated with an adequate trial of SSRIs previously within two years prior to enrollment. The age at onset was 58 ± 11 years (range 33-75 years) and the duration of the present episode was 14 ± 10 months (range 2 to 36 months). One of the controls and none of the LLD patients were left-handed. The groups did not significantly differ in age, sex distributions, nor on baseline neuropsychological measures ($P > 0.05$). One LLD patient received a CDR score of 0.5 (mild cognitive impairment [MCI]). All other subjects received a CDR score of 0 (normal). As expected, the LLD group had significantly higher HAMD and BDI scores at baseline (F (1, 39) = 839.95; $P = 0.000$); F (1, 39) =30.53, $P = 0.000$, respectively).

10

3.2 Clinical and Neuropsychological Effects of SSRI Treatment: All but one LLD patient completed the follow-up clinical and neuropsychological assessments and 5-HTT scan. Sixteen LLD patients were treated with Citalopram and three were treated with Sertraline. The Sertraline treated patients were included in all analyses except for the association between 5-HTT occupancy and plasma Citalopram concentrations. At the time of the follow-up 5-HTT PET scan, the mean Citalopram dose was 21mg ± 9mg (range 10-40mg) and the mean Sertraline dose was 92mg ± 52mg (range 50-150mg). One LLD patients was treated with Citalopram at the time of the "black box" warning. The patient responded to the 20mg dose and was able to remain on Citalopram treatment as she did not require a further dose increase. Side effects were not reported in the LLD patients. SSRI treatment significantly improved depressive symptoms (HAMD: $F_{(1, 18)} = 205.6$; $p = 0.000$); BDI: $F_{(1, 18)} = 38.00$, $p = 0.000$; Table 1). The magnitude of change in the HAMD was a mean of $-12 ± 4$ (range -1 to -17) and in the BDI was a mean of $-15 ± 10$ (range -1 to -32). Eighteen of the 19 patients were treatment responders. The number of LLD patients who met response criteria at the following times are: 2 at week 4, 7 at week 6, 7 at week 8, 2 at week 10 and 1 at week 12. Only the two visual-spatial memory tests showed significant improvement with SSRI treatment. The BVMT-R sum of the first three trials and delayed recall measures increased significantly ($F_{(1, 19)} = 7.53$, $P = 0.013$; $F_{(1, 19)} = 14.06$, $P < 0.001$). The Rey Complex Figure immediate and delayed recall, but not the copy condition showed significant increases ($F_{(1, 19)} = 33.80$, $P = 0.000$; $F_{(1, 19)} = 61.10$, $P = 0.00$; $F_{(1, 19)} = 1.56$; $P = 0.228$). There was no statistically significant change in the other neuropsychological measures with SSRI treatment.

3.3 5-HTT Availability, Correlations with Mood and Neuropsychological Outcomes and Grey Matter Volumes: The VOI results demonstrated significantly lower 5-HTT availability in the caudate [$F_{(1,39)} = 4.16$; $P = 0.048$], hippocampus [$F_{(1,39)} = 4.88$; $P = 0.033$], entorhinal cortex [$F_{(1,39)} = 15.03$; $P = 0.000$] and parahippocampal gyrus [$F_{(1,39)} = 7.18$; $P = 0.011$] (Table 2). The other VOIs did not demonstrate significant between group differences. In the analysis of between-group differences in 5-HTT availability in the VOIs subdivided by Braak stages, significant differences in Stage I and Stage II only were observed (entorhinal cortex and hippocampus, respectively), $F_{(1, 39)} = 15.03$; $P = 0.001$ and $F_{(1, 39)} = 4.88$; $P = 0.033$; Table 3). 5-HTT availability was lower in the LLD patients relative to controls in Stages II to IV and comparable between-groups in Stages V and VI. The exploratory, voxel-wise analyses demonstrated that the LLD patients relative to controls had lower 5-HTT availability in the left lateral orbital gyrus (BA 11), right insula, left superior (BA 22, 38), right middle (BA 21) and bilateral inferior (BA 20) temporal gyri (BA 22, 21, 20), bilateral parahippocampal gyri (BA 36), right amygdala, and bilateral fusiform gyri (BA 37 left and BA 20 right; Table 4; Figure 1). Moreover, 5-HTT availability was lower in the left amygdala and left hippocampus at $p \leq 0.002$, just below the statistical threshold set for this comparison. No regions demonstrated greater 5-HTT availability in the LLD patients relative to the controls. There were no significant correlations observed between baseline 5-HTT availability and the baseline clinical and neuropsychological measures. Likewise, there was no significant

11

correlation between pre-treatment 5-HTT availability and change in the clinical and neuropsychological measures with SSRI treatment in the LLD patients. There was no significant between-group difference in gray matter volumes.

3.4 5-HTT Occupancy and the Relationship to Plasma Citalopram Concentrations: Significant 5-HTT occupancy with SSRI treatment was observed in the cingulate gyrus (BA 23, 24, 32), superior frontal gyrus (BA 10), left medial and orbital gyrus (BA 10, 11), insula (BA 13), superior temporal (BA 38), right middle temporal gyrus (BA 20) and right inferior temporal gyri (BA 38), parahippocampal gyrus (BA 36), amygdala, hippocampus, post-central gyrus (BA1), precuneus (BA 23), fusiform (BA 37), left supramarginal gyrus (BA 41), right pericalcarine gyrus (BA 17, 23), right lingual gyrus (BA 18), cuneus (BA 18), left caudate, ventral striatum, putamen and thalamus (bilateral unless otherwise noted; Supplemental Table 1; Figure 2).

Regional 5-HTT occupancy relative to plasma Citalopram concentrations was calculated (Table 5; Figure 3). In the majority of the aforementioned regions, 5-HTT occupancy was greater than 70% across a range of observed Citalopram plasma concentrations (28 – 117 ng/mL). In fact, the no change model ($y = c$) showed a better fit than the linear model ($y = a \cdot x + b$; $p > 0.06$). Accordingly, the data fit better when O_{max} was estimated together with IC_{50} than when IC_{50} alone was fitted with O_{max} set at 100%, as exemplified for the thalamus (Figure 2). Estimates of O_{max} ranged from 60 - 97% across regions (Table 3). These observations suggested that 5-HTT were almost saturated by Citalopram in these regions, close to the maximal occupancy (mean occupancy over O_{max}; over 95% in some regions). In sum, commonly used doses of Citalopram resulted in plasma concentrations that were several-fold greater than observed values of IC_{50} and occupancies exceeding 85% (>> 50%). For this reason, it appeared IC_{50} had little clinical significance for Citalopram aside from being necessary for defining the prediction model.

3.5 Correlations between 5-HTT Occupancy and Mood and Cognitive Outcomes: Among the LLD patients, both depression scales (HAMD and BDI) showed significant improvement with SSRI treatment. However, 5-HTT occupancy with SSRI treatment correlated with improvement in depressive symptoms only with the BDI, possibly due to the greater variability in response of the BDI compared to the HAMD (Table 6a; Supplemental Figure 1). Greater BDI improvement correlated with greater 5-HTT occupancy in a limited number of brain regions, including the left paracentral lobule (BA 5) and bilateral posterior cingulate gyrus (BA 31). Among the five neuropsychological tests that were improved by SSRI treatment, correlations with 5-HTT occupancy were performed for the CVLT (total words recalled in the first 5 trials), BVMT-R (total shapes recalled in the first three trials) and the verbal fluency (letter and category) tests. Only improvement in BVMT-R was correlated with 5-HTT occupancy. Correlations were observed in the bilateral insula (BA 13), right superior, middle and inferior temporal gyri (BA 22, 22, 20), bilateral transverse temporal gyri (BA 40/BA41), bilateral precuneus (BA 23), bilateral posterior cingulate gyri (BA 23), bilateral fusiform gyrus (BA 37), bilateral supramarginal gyri (BA

12

40), right pericalcarine gyrus (BA 17), isthmus/cingulate (BA 18), right lingual gyrus (BA 18), left hippocampus, bilateral putamen, right globus pallidus and bilateral thalamus (Table 6b).

4.0 Discussion

The LLD patients relative to controls had lower 5-HTT availability in lateral frontal, insula, temporal and parietal cortices, amygdala, entorhinal cortex, parahippocampal gyrus and hippocampus based upon VOI and exploratory, voxel-wise analyses. The reduction in 5-HTT availability was observed in the absence of significant between-group differences in gray matter volumes, suggesting that serotonin degeneration may be observed before widespread neuronal loss. The lack of a difference between LLD patients and controls in gray matter volumes is consistent with some published studies (as reviewed by Jamieson et al., 2019). Lower 5-HTT availability in the LLD patients relative to controls is observed in contrast to the lack of a between-group difference reported in serotonin (5-HT1A and 5-HT2A) receptors (Meltzer et al., 2004, 1999). 5-HTT is a more specific marker of serotonin degeneration than the 5-HT1A or 5-HT2A receptors that are located on the terminals of non-serotonergic neurons (Azmitia and Nixon, 2008). Lower 5-HTT in LLD patients relative to controls indicates either less serotonin innervation or greater 5-HTT internalization secondary to lower intrasynaptic serotonin levels (Kovachich et al., 1988; Underwood et al., 2018). Relatively normal levels of serotonin receptors, in the face of decreased 5-HTT availability, implicates a relatively early stage of serotonin neurodegeneration that does not yet involve a compensatory serotonin receptor upregulation. Decreases in 5-HTT availability might reflect a developing axonal pathology that is known to precede serotonergic neuron loss (Wihan et al., 2019).

Neuropathological and neuroimaging studies using SSRI analogs as radiologands/radiotracers (respectively) to measure 5-HT in patients with midlife, unipolar major depression (non-suicidal) relative to controls have shown mixed results. These studies, as well as neuroimaging studies have found increases, decreases or no change in 5-HTT in patients relative to controls (as reviewed by Spies et al., 2015; Underwood et al., 2018). While the direction of the results varies across studies, the regions implicated are consistent and cingulate gyrus, frontal cortex, amygdala, thalamus and striatum (Spies et al., 2015). The one post-mortem study of 5-HTT in LLD patients did not detect a decrease relative to controls in the prefrontal cortex (Thomas et al., 2006).

In contrast to mid-life depressed patients, the present study revealed decreased 5-HTT availability mainly in temporal and parietal cortical and limbic regions in LLD patients relative to controls. These regional changes overlap to some extent with the decreased 5-HTT availability observed in individuals with MCI relative to controls (Smith et al., 2017). However, lower 5-HTT availability reported in MCI relative to controls is greater in magnitude and is more extensive as additional frontal cortical, limbic and subcortical regions are involved compared to the decreases observed in the LLD patients relative to controls. The pathophysiology of lower 5-

13

HTT availability, reflecting decreased serotonin innervation or endogenous serotonin levels, may be different in LLD compared to mid-life depressed patients and may be associated with an aging-related neurodegenerative process in LLD patients. For example, tau deposition is found in the dorsal raphe in the early Braak stages in preclinical AD and early AD patients and then, spreads to the other raphe nuclei and cortical regions in the later Braak stages (Rüb et al., 2000; Simic et al., 2010). In the present study, significant decreases in 5-HTT was observed in regions that comprise the earliest Braak stages (Stage I- entorhinal cortex). Multi-modality molecular imaging studies of the neurobiological mechanisms associated with serotonin degeneration (e.g. tau, amyloid and neuroinflammation) may also explain the variability in depressive and cognitive responses to antidepressants.

There was no significant correlation in this study between baseline 5-HTT availability and baseline (patients and controls) or change in depressive symptoms or cognitive function (patients only). The lack of correlation between depressive symptoms and 5-HTT prior to treatment is consistent with observations made in the majority of studies in mid-life depressed patients (Ichimiya et al., 2002; Meyer et al., 2004; Miller et al., 2013; Parsey et al., 2006a). The lack of correlation between baseline 5-HTT availability and the neuropsychological measures may be due to the fact that the LLD patients did not have significant cognitive impairment. In contrast, correlations were observed between 5-HTT occupancy and change in depressive symptoms and neuropsychological outcomes.

In the present study, the magnitude of 5-HTT occupancy by SSRI's was greater than 70% for all regions (except for the posterior cingulate) and over 80% for most regions. The majority of studies in controls and mid-life depressed patients have shown 70% or greater occupancy in the striatum and thalamus, to a greater extent after chronic rather than acute treatment (Lundberg et al., 2012; Meyer et al., 2004; Meyer et al., 2001). Thus, the magnitude of 5-HTT occupancy in LLD patients is comparable and even greater than that observed in mid-life depressed patients. In the LLD patients, regional 5-HTT occupancy by SSRIs was observed in cortical and subcortical regions, including frontal, temporal, parietal and association areas, as well as primary sensory areas. 5-HTT occupancy was observed in the amygdala and hippocampus, as well as subcortical regions including the ventral striatum, putamen and thalamus. The regional pattern of 5-HTT occupancy observed in LLD patients was similar to that observed in a previous study of mid-life depressed patients who were scanned after 3 weeks of treatment with Citalopram or Escitalopram, (Baldinger et al., 2014), as well as a previous study in LLD patients employing voxel-wise analysis methods (Smith et al., 2011). The sample size in the present study is comparable to the majority serotonin transporter imaging and occupancy studies that have had a sample size of approximately 20 subjects or less. Several papers report data from larger samples of patients treated with different antidepressants for comparison (as reviewed by (Arakawa et al., 2020; Spies et al., 2015).

14

The LLD patients in this study demonstrated improvement in depressive symptoms and visual-spatial memory with SSRI treatment. Correlations with depressive symptoms were limited to paracentral lobule and posterior cingulate and were also observed in temporal and parietal cortices and hippocampus, but not at a cluster-wise corrected level. A study of mid-life depressed patients treated with SSRIs for three weeks demonstrated significant voxel-wise correlations between improvement in depressive symptoms and greater 5-HTT occupancy in anterior and sub-genual cingulate, medial orbitofrontal cortex, habenula, amygdala, angular gyrus, putamen and anterior midbrain (Lanzenberger et al., 2012). Correlations between improved cognition with SSRI treatment and 5-HTT occupancy has not been the focus of prior studies. The improvement in visual-spatial memory with antidepressant treatment in LLD patients, including the tests administered in the present study, has been reported previously (Barch et al., 2012). Improvement in visual-spatial memory performance correlated with 5-HTT occupancy in temporal and parietal cortices, hippocampus, striatum and thalamus. These are regions that have been implicated in visual-spatial memory performance and are representative of regions that show correlations between 5-HTT and visual-spatial memory performance in individuals with MCI (Smith et al., 2017). These regions of correlation between 5-HTT occupancy and improvement in depressive symptoms and visual-spatial memory were similar to the cortical and limbic regions that showed decreases in cerebral glucose metabolism by Citalopram in LLD patients (Diaconescu et al., 2011; Smith et al., 2009). To more conclusively establish the role of 5-HTT occupancy in treatment response, LLD patients with more severe depressive symptoms and cognitive deficits and a history of variability in treatment response should be studied. It is noteworthy that significant correlations were observed, given the relatively narrow range of regional 5-HTT occupancies (70-99%). High levels of 5-HTT occupancy may be relevant to greater mood and neuropsychological outcomes. As the magnitude of regional 5-HTT occupancies did not depend on plasma SSRI levels (high levels of occupancy were observed at relatively low plasma concentrations), other factors may contribute to variability in the observed range of 5-HTT occupancy (e.g. serotonin transporter promoter polymorphisms, drug metabolism), as well as other neurobiological effects of SSRIs that might affect treatment response (Marshe et al., 2020; Smith et al., 2004).

In conclusion, decreased 5-HTT availability in LLD patients relative to controls was observed that may reflect an early stage of serotonin degeneration in LLD patients. The results also support the role of 5-HTT occupancy in the response of depression and neuropsychological responses to SSRI treatment. Other serotonergic therapeutic targets may be even more effective in treating LLD and associated cognitive deficits, particularly treatments that target the pre- and post-synaptic receptors that may not be as affected as 5-HTT (Meltzer et al., 2004, 1999). Preclinical studies show that SSRIs and serotonergic receptor compounds (5-HT4 agonists and 5-HT6 antagonists) may have effects on neurodegenerative processes such as blocking amyloid precursor protein processing and tau deposition, as well as improving both depressive symptoms and cognitive deficits (Mattson et al., 2004; Meneses, 2016; Nelson et al., 2007). Serotonergic treatments may have potential benefit

15

in treating and preventing depressive symptoms and cognitive deficits through multiple, relevant, neurochemical and molecular mechanisms.

REFERENCES

Akaike, H., 1974. A New Look at the Statistical Model Identification. IEEE Trans. Automat. Contr. https://doi.org/10.1109/TAC.1974.1100705

Alexopoulos, G.S., Meyers, B.S., Young, R.C., Mattis, S., Kakuma, T., 1993. The course of geriatric depression with "reversible dementia": A controlled study. Am. J. Psychiatry 150, 1693–1699. https://doi.org/10.1176/ajp.150.11.1693

Alexopoulos, G.S., Vrontou, C., Kakuma, T., Meyers, B.S., Young, R.C., Klausner, E., Clarkin, J., 1996. Disability in geriatric depression. Am. J. Psychiatry. https://doi.org/10.1176/ajp.153.7.877

Arakawa, R., Takano, A., Halldin, C., 2020. PET technology for drug development in psychiatry. Neuropsychopharmacol. Reports. https://doi.org/10.1002/npr2.12084

Ashburner, J., 2007. A fast diffeomorphic image registration algorithm. Neuroimage. https://doi.org/10.1016/j.neuroimage.2007.07.007

Azmitia, E.C., Nixon, R., 2008. Dystrophic serotonergic axons in neurodegenerative diseases. Brain Res. https://doi.org/10.1016/j.brainres.2008.03.060

Baldinger, P., Kranz, G.S., Haeusler, D., Savli, M., Spies, M., Philippe, C., Hahn, A., Höflich, A., Wadsak, W., Mitterhauser, M., Lanzenberger, R., Kasper, S., 2014. Regional differences in SERT occupancy after acute and prolonged SSRI intake investigated by brain PET. Neuroimage. https://doi.org/10.1016/j.neuroimage.2013.10.002

Barch DM, D'Angelo G, Pieper C, Wilkins CH, Welsh-Bohmer K, Taylor W, Garcia KS, Gersing K, Doraiswamy PM, Sheline YI.Cognitive improvement following treatment in late-life depression: relationship to vascular risk and age of onset. Am J Geriatr Psychiatry. 2012 Aug;20(8):682-90. doi: 10.1097/JGP.0b013e318246b6cb.

Bechara, A., 2007. Iowa Gambling Task Professional Manual, Psychological Assessment Resources, Inc.

Beck, A.T., Steer, R.A., 1993. Manual for the Beck Depression Inventory. San Antonio, TX Psychol. Corp.

Benedict, R.H.B., 1997. Brief Visuospatial Memory Test - Revised: Professional manual. Psychological Assessment Resources, Inc, Odessa, FL.

Bhalla, R.K., Butters, M.A., Mulsant, B.H., Begley, A.E., Zmuda, M.D., Schoderbek, B., Pollock, B.G., Reynolds, C.F., Becker, J.T., 2006. Persistence of neuropsychologic deficits in the remitted state of late-life depression. Am. J. Geriatr. Psychiatry. https://doi.org/10.1097/01.JGP.0000203130.45421.69

Boyce, R.D., Handler, S.M., Karp, J.F., Hanlon, J.T., 2012. Age-related changes in antidepressant pharmacokinetics and potential drug-drug interactions: A comparison of evidence-based literature and package insert information. Am. J. Geriatr. Pharmacother.

16

https://doi.org/10.1016/j.amjopharm.2012.01.001

Braak, H., Braak, E., 1991. Neuropathological stageing of Alzheimer-related changes. Acta Neuropathol. https://doi.org/10.1007/BF00308809

Bruce, M.L., Leaf, P.J., 1989. Psychiatric disorders and 15-month mortality in a community sample of older adults. Am. J. Public Health. https://doi.org/10.2105/AJPH.79.6.727

Butters, M.A., Bhalla, R.K., Mulsant, B.H., Mazumdar, S., Houck, P.R., Begley, A.E., Dew, M.A., Pollock, B.G., Nebes, R.D., Becker, J.T., Reynolds, C.F., 2004a. Executive functioning, illness course, and relapse/recurrence in continuation and maintenance treatment of late-life depression: Is there a relationship? Am. J. Geriatr. Psychiatry. https://doi.org/10.1097/00019442-200407000-00006

Butters, M.A., Whyte, E.M., Nebes, R.D., Begley, A.E., Dew, M.A., Mulsant, B.H., Zmuda, M.D., Bhalla, R., Meltzer, C.C., Pollock, B.G., Reynolds, C.F., Becker, J.T., 2004b. The nature and determinants of neuropsychological functioning in late-life depression. Arch. Gen. Psychiatry. https://doi.org/10.1001/archpsyc.61.6.587

Coppen, A., 1967. The biochemistry of affective disorders. Br. J. Psychiatry. https://doi.org/10.1192/bjp.113.504.1237

Delis, D., Kramer, J., Kaplan, E., Ober, B., 1987. California Verbal Learning Test (CVLT) Manual. Psychol. Corp. https://doi.org/10.1207/s15328023top2503_18

Delis, D.C., Kaplan, E., Kramer, J.H., 2006. Delis Kaplan Executive Function System (D-KEFS) Test Review. Appl. Neuropsychol.

Desikan, R.S., Ségonne, F., Fischl, B., Quinn, B.T., Dickerson, B.C., Blacker, D., Buckner, R.L., Dale, A.M., Maguire, R.P., Hyman, B.T., Albert, M.S., Killiany, R.J., 2006. An automated labeling system for subdividing the human cerebral cortex on MRI scans into gyral based regions of interest. Neuroimage. https://doi.org/10.1016/j.neuroimage.2006.01.021

Dew, M.A., Reynolds, C.F., Houck, P.R., Hall, M., Buysse, D.J., Frank, E., Kupfer, D.J., 1997. Temporal profiles of the course of depression during treatment: Predictors of pathways toward recovery in the elderly. Arch. Gen. Psychiatry. https://doi.org/10.1001/archpsyc.1997.01830230050007

Diaconescu, A.O., Kramer, E., Hermann, C., Ma, Y., Dhawan, V., Chaly, T., Eidelberg, D., Mcintosh, A.R., Smith, G.S., 2011a. Distinct functional networks associated with improvement of affective symptoms and cognitive function during citalopram treatment in geriatric depression. Hum. Brain Mapp. 32, 1677–1691. https://doi.org/10.1002/hbm.21135

Diniz, B.S., Butters, M.A., Albert, S.M., Dew, M.A., Reynolds, C.F., 2013. Late-life depression and risk of vascular dementia and Alzheimer's disease: Systematic review and meta-analysis of community-based cohort studies. Br. J. Psychiatry. https://doi.org/10.1192/bjp.bp.112.118307

First, M., Spitzer, R., Gibbon, M., Williams, J., Davies, Borus, J., Howes, M.J., Kane, J., Pope, H.G., Rounsaville, B., 1995. The Structured Clinical Interview for DSM-IV Axis I Disorders-Patient Edition, Biometrics Research Department. https://doi.org/10.1521/pedi.1995.9.2.92

17

Fischl, B., Salat, D.H., Busa, E., Albert, M., Dieterich, M., Haselgrove, C., Van Der Kouwe, A., Killiany, R., Kennedy, D., Klaveness, S., Montillo, A., Makris, N., Rosen, B., Dale, A.M., 2002. Whole brain segmentation: Automated labeling of neuroanatomical structures in the human brain. Neuron. https://doi.org/10.1016/S0896-6273(02)00569-X

Folstein, M.F., Folstein, S.E., McHugh, P.R., 1975. "Mini-mental state". A practical method for grading the cognitive state of patients for the clinician. J. Psychiatr. Res. https://doi.org/10.1016/0022-3956(75)90026-6

Guy, W., 2008. Clinical Global Impressions (CGI) Scale. Handb. Psychiatr. Meas.

HAMILTON, M., 1960. A rating scale for depression. J. Neurol. Neurosurg. Psychiatry. https://doi.org/10.1136/jnnp.23.1.56

Ichimiya, T., Suhara, T., Sudo, Y., Okubo, Y., Nakayama, K., Nankai, M., Inoue, M., Yasuno, F., Takano, A., Maeda, J., Shibuya, H., 2002. Serotonin transporter binding in patients with mood disorders: A PET study with [11C](+)McN5652. Biol. Psychiatry. https://doi.org/10.1016/S0006-3223(01)01351-8

Ichise, M., Liow, J.S., Lu, J.Q., Takano, A., Model, K., Toyama, H., Suhara, T., Suzuki, K., Innis, R.B., Carson, R.E., 2003. Linearized reference tissue parametric imaging methods: Application to [11C]DASB positron emission tomography studies of the serotonin transporter in human brain. J. Cereb. Blood Flow Metab. https://doi.org/10.1097/01.WCB.0000085441.37552.CA

Innis, R.B., Cunningham, V.J., Delforge, J., Fujita, M., Gjedde, A., Gunn, R.N., Holden, J., Houle, S., Huang, S.C., Ichise, M., Iida, H., Ito, H., Kimura, Y., Koeppe, R.A., Knudsen, G.M., Knuuti, J., Lammertsma, A.A., Laruelle, M., Logan, J., Maguire, R.P., Mintun, M.A., Morris, E.D., Parsey, R., Price, J.C., Slifstein, M., Sossi, V., Suhara, T., Votaw, J.R., Wong, D.F., Carson, R.E., 2007. Consensus nomenclature for in vivo imaging of reversibly binding radioligands. J. Cereb. Blood Flow Metab. https://doi.org/10.1038/sj.jcbfm.9600493

Jamieson, A., Goodwill, A.M., Termine, M., Campbell, S., Szoeke, C., 2019. Depression related cerebral pathology and its relationship with cognitive functioning: A systematic review. J. Affect. Disord. 250, 410–418. https://doi.org/10.1016/j.jad.2019.03.042

Jorm, A.F., Van Duijn, C.M., Chandra, V., Fratiglioni, L., Graves, A., Heyman, A., Kokmen, E., Kondo, Mortimer, J.A., Rocca, W.A., Shalat, S.L., Soininen, H., Hofman, A., 1991. Psychiatric history and related exposures as risk factors foralzheimer's disease: A collaborativere-analysis of case-control studies. Int. J. Epidemiol. https://doi.org/10.1093/ije/20.Supplement_2.S43

Kovachich, G.B., Aronson, C.E., Brunswick, D.J., Frazer, A., 1988. Quantitative autoradiography of serotonin uptake sites in rat brain using [3H]cyanoimipramine. Brain Res. https://doi.org/10.1016/0006-8993(88)90805-0

Kumar, J.S., Mann, J., 2014. PET Tracers for Serotonin Receptors and Their Applications. Cent. Nerv. Syst. Agents Med. Chem. https://doi.org/10.2174/1871524914666141030124316

Lacadie, C.M., Fulbright, R.K., Rajeevan, N., Constable, R.T., Papademetris, X., 2008. More accurate

Talairach coordinates for neuroimaging using non-linear registration. Neuroimage. https://doi.org/10.1016/j.neuroimage.2008.04.240

Lanzenberger, R., Kranz, G.S., Haeusler, D., Akimova, E., Savli, M., Hahn, A., Mitterhauser, M., Spindelegger, C., Philippe, C., Fink, M., Wadsak, W., Karanikas, G., Kasper, S., 2012. Prediction of SSRI treatment response in major depression based on serotonin transporter interplay between median raphe nucleus and projection areas. Neuroimage. https://doi.org/10.1016/j.neuroimage.2012.07.023

Lockwood, K.A., Alexopoulos, G.S., Van Gorp, W.G., 2002. Executive dysfunction in geriatric depression. Am. J. Psychiatry. https://doi.org/10.1176/appi.ajp.159.7.1119

Logan, J., Fowler, J.S., Volkow, N.D., Wang, G.J., Ding, Y.S., Alexoff, D.L., 1996. Distribution volume ratios without blood sampling from graphical analysis of PET data. J. Cereb. Blood Flow Metab. https://doi.org/10.1097/00004647-199609000-00008

Lundberg, J., Tiger, M., Landén, M., Halldin, C., Farde, L., 2012. Serotonin transporter occupancy with TCAs and SSRIs: A PET study in patients with major depressive disorder. Int. J. Neuropsychopharmacol. https://doi.org/10.1017/S1461145711001945

Marshe, V.S., Islam, F., Maciukiewicz, M., Bousman, C., Eyre, H.A., Lavretsky, H., Mulsant, B.H., Reynolds, C.F., Lenze, E.J., Müller, D.J., 2020. Pharmacogenetic Implications for Antidepressant Pharmacotherapy in Late-Life Depression: A Systematic Review of the Literature for Response, Pharmacokinetics and Adverse Drug Reactions. Am. J. Geriatr. Psychiatry. https://doi.org/10.1016/j.jagp.2020.01.007

Mattson, M.P., Maudsley, S., Martin, B., 2004. BDNF and 5-HT: A dynamic duo in age-related neuronal plasticity and neurodegenerative disorders. Trends Neurosci. https://doi.org/10.1016/j.tins.2004.08.001

Meltzer, C.C., Price, J.C., Mathis, C.A., Butters, M.A., Ziolko, S.K., Moses-Kolko, E., Mazumdar, S., Mulsant, B.H., Houck, P.R., Lopresti, B.J., Weissfeld, L.A., Reynolds, C.F., 2004. Serotonin IA receptor binding and treatment response in late-life depression. Neuropsychopharmacology. https://doi.org/10.1038/sj.npp.1300556

Meltzer, C.C., Price, J.C., Mathis, C.A., Greer, P.J., Cantwell, M.N., Houck, P.R., Mulsant, B.H., Ben-Eliezer, D., Lopresti, B., DeKosky, S.T., Reynolds, C.F., 1999. PET imaging of serotonin type 2A receptors in late-life neuropsychiatric disorders. Am. J. Psychiatry. https://doi.org/10.1176/ajp.156.12.1871

Meneses, A., 2016. Neural activity, memory, and dementias: Serotonergic markers. Behav. Pharmacol. https://doi.org/10.1097/FBP.0000000000000279

Meyer, J. H., Houle, S., Sagrati, S., Carella, A., Hussey, D.F., Ginovart, N., Goulding, V., Kennedy, J., Wilson, A.A., 2004. Brain Serotonin Transporter Binding Potential Measured With Carbon11–Labeled DASB Positron Emission Tomography. Arch. Gen. Psychiatry 61, 1271. https://doi.org/10.1001/archpsyc.61.12.1271

Meyer, J.H., Wilson, A.A., Ginovart, N., Goulding, V., Hussey, D., Hood, K., Houle, S., 2001. Occupancy of serotonin transporters by paroxetine and citalopram during treatment of depression: A [11C]DASB PET imaging study. Am. J. Psychiatry. https://doi.org/10.1176/appi.ajp.158.11.1843

19

Meyer, J. H, Wilson, A.A., Sagrati, S., Hussey, D., Carella, A., Potter, W.Z., Ginovart, N., Spencer, E.P., Cheok, A., Houle, S., 2004. Serotonin Transporter Occupancy of Five Selective Serotonin Reuptake Inhibitors at Different Doses: An. Am. J. Psychiatry.

Miller, J.M., Hesselgrave, N., Ogden, R.T., Sullivan, G.M., Oquendo, M.A., Mann, J.J., Parsey, R. V., 2013. Positron emission tomography quantification of serotonin transporter in suicide attempters with major depressive disorder. Biol. Psychiatry. https://doi.org/10.1016/j.biopsych.2013.01.024

Morris, JC. 1993. The Clinical Dementia Rating (CDR): current version and scoring rules. Neurol 43, 2412–2414.

Nelson, R.L., Guo, Z., Halagappa, V.M., Pearson, M., Gray, A.J., Matsuoka, Y., Brown, M., Martin, B., Iyun, T., Maudsley, S., Clark, R.F., Mattson, M.P., 2007. Prophylactic treatment with paroxetine ameliorates behavioral deficits and retards the development of amyloid and tau pathologies in 3xTgAD mice. Exp. Neurol. https://doi.org/10.1016/j.expneurol.2007.01.037

Ownby, R.L., Crocco, E., Acevedo, A., John, V., Loewenstein, D., 2006. Depression and risk for Alzheimer disease: Systematic review, meta-analysis, and metaregression analysis. Arch. Gen. Psychiatry. https://doi.org/10.1001/archpsyc.63.5.530

Øyehaug, E., Østensen, E.T., Salvesen, B., 1982. Determination of the antidepressant agent citalopram and metabolites in plasma by liquid chromatography with fluorescence detection. J. Chromatogr. B Biomed. Sci. Appl. https://doi.org/10.1016/S0378-4347(00)80362-X

Parsey, R. V., Hastings, R.S., Oquendo, M.A., Huang, Y.Y., Simpson, N., Arcement, J., Huang, Y., Ogden, R.T., Van Heertum, R.L., Arango, V., Mann, J.J., 2006a. Lower serotonin transporter binding potential in the human brain during major depressive episodes. Am. J. Psychiatry. https://doi.org/10.1176/appi.ajp.163.1.52

Parsey, R. V., Kent, J.M., Oquendo, M.A., Richards, M.C., Pratap, M., Cooper, T.B., Arango, V., Mann, J.J., 2006b. Acute Occupancy of Brain Serotonin Transporter by Sertraline as Measured by [11C]DASB and Positron Emission Tomography. Biol. Psychiatry. https://doi.org/10.1016/j.biopsych.2005.08.010

Rahmim, A., Cheng, J.C., Blinder, S., Camborde, M.L., Sossi, V., 2005. Statistical dynamic image reconstruction in state-of-the-art high-resolution PET. Phys. Med. Biol. https://doi.org/10.1088/0031-9155/50/20/010

Rey, A., 1941. L'examen psychologique dans les cas d'encephalopathie traumatique (Psychological examination of brain damage cases). Arch. Psychol. (Geneve).

Rüb, U., Del Tredici, K., Schultz, C., Thal, D.R., Braak, E., Braak, H., 2000. The evolution of Alzheimer's disease-related cytoskeletal pathology in the human raphe nuclei. Neuropathol. Appl. Neurobiol. https://doi.org/10.1046/j.0305-1846.2000.00291.x

Sackeim HA. The definition and meaning of treatment-resistant depression.J Clin Psychiatry. 2001;62 Suppl 16:10-7.

Schildkraut, J.J., 1965. The catecholamine hypothesis of affective disorders: a review of supporting evidence.

20

Am. J. Psychiatry. https://doi.org/10.1176/ajp.122.5.509

Schöll, M., Lockhart, S.N., Schonhaut, D.R., O'Neil, J.P., Janabi, M., Ossenkoppele, R., Baker, S.L., Vogel, J.W., Faria, J., Schwimmer, H.D., Rabinovici, G.D., Jagust, W.J., 2016. PET Imaging of Tau Deposition in the Aging Human Brain. Neuron. https://doi.org/10.1016/j.neuron.2016.01.028

Simic, G., Stani, G., Mladinov, M., Jovanov-milosevic, N., Hof, P.R., 2010. Does Alzheimer's disease begin in the brainstem. Neuropathol. Appl. Neurobiol. https://doi.org/10.1111/j.1365-2990.2009.01038.x.Annotation

Smith, A., 1968. The Symbol-Digit Modalities Test: A neuropsychologic test for economic screening of learning and other cerebral disorders. Learn. Disord.

Smith, G.S., Barrett, F.S., Joo, J.H., Nassery, N., Savonenko, A., Sodums, D.J., Marano, C.M., Munro, C.A., Brandt, J., Kraut, M.A., Zhou, Y., Wong, D.F., Workman, C.I., 2017. Molecular imaging of serotonin degeneration in mild cognitive impairment. Neurobiol. Dis. 105. https://doi.org/10.1016/j.nbd.2017.05.007

Smith, G.S., Kahn, A., Sacher, J., Rusjan, P., Van Eimeren, T., Flint, A., Wilson, A.A., 2011. Serotonin transporter occupancy and the functional neuroanatomic effects of citalopram in geriatric depression. Am. J. Geriatr. Psychiatry 19. https://doi.org/10.1097/JGP.0b013e318227f83f

Smith, G.S., Kramer, E., Hermann, C., Ma, Y., Dhawan, V., Chaly, T., Eidelberg, D., 2009. Serotonin Modulation of Cerebral Glucose Metabolism in Depressed Older Adults. Biol. Psychiatry. https://doi.org/10.1016/j.biopsych.2009.02.012

Smith, G.S., Lotrich, F.E., Malhotra, A.K., Lee, A.T., Ma, Y., Kramer, E., Gregersen, P.K., Eidelberg, D., Pollock, B.G., 2004. Effects of serotonin transporter promoter polymorphisms on serotonin function. Neuropsychopharmacology 29. https://doi.org/10.1038/sj.npp.1300552

Sossi, V., De Jong, H.W.A.M., Barker, W.C., Bloomfield, P., Burbar, Z., Camborde, M.L., Comtat, C., Eriksson, L.A., Houle, S., Keator, D., Knöß, C., Krais, R., Lammertsma, A.A., Rahmim, A., Sibomana, M., Teräs, M., Thompson, C.J., Trébossen, R., Votaw, J., Walker, M., Wienhard, K., Wong, D.F., 2005. The second generation HRRT - A multi-centre scanner performance investigation, in: IEEE Nuclear Science Symposium Conference Record. https://doi.org/10.1109/NSSMIC.2005.1596770

Spies, M., Knudsen, G.M., Lanzenberger, R., Kasper, S., 2015. The serotonin transporter in psychiatric disorders: Insights from PET imaging. The Lancet Psychiatry. https://doi.org/10.1016/S2215-0366(15)00232-1

Suckow, R.F., Ming Fen Zhang, Cooper, T.B., 1992. Sensitive and selective liquid-chromatographic assay of fluoxetine and norfluoxetine in plasma with fluorescence detection after precolumn derivatization. Clin. Chem. https://doi.org/10.1093/clinchem/38.9.1756

Thomas, A.J., Hendriksen, M., Piggott, M., Ferrier, I.N., Perry, E., Ince, P., O'Brien, J.T., 2006. A study of the serotonin transporter in the prefrontal cortex in late-life depression and Alzheimer's disease with and without depression. Neuropathol. Appl. Neurobiol. https://doi.org/10.1111/j.1365-2990.2006.00728.x

Trillo, L., Das, D., Hsieh, W., Medina, B., Moghadam, S., Lin, B., Dang, V., Sanchez, M.M., De Miguel, Z.,

21

Ashford, J.W., Salehi, A., 2013. Ascending monoaminergic systems alterations in Alzheimer's disease. Translating basic science into clinical care. Neurosci. Biobehav. Rev. https://doi.org/10.1016/j.neubiorev.2013.05.008

Underwood, M.D., Kassir, S.A., Bakalian, M.J., Galfalvy, H., Dwork, A.J., Mann, J.J., Arango, V., 2018. Serotonin receptors and suicide, major depression, alcohol use disorder and reported early life adversity. Transl. Psychiatry. https://doi.org/10.1038/s41398-018-0309-1

Varnäs, K., Halldin, C., Hall, H., 2004. Autoradiographic distribution of serotonin transporters and receptor subtypes in human brain. Hum. Brain Mapp. https://doi.org/10.1002/hbm.20035

Vieweg, W.V.R., Hasnain, M., Howland, R.H., Hettema, J.M., Kogut, C., Wood, M.A., Pandurangi, A.K., 2012. Citalopram, QTc interval prolongation, and torsade de pointes. How should we apply the recent FDA ruling? Am. J. Med. https://doi.org/10.1016/j.amjmed.2011.12.002

Wechsler, D., 1997. Wechsler memory scale - Third edition administration and scoring manual. San Antonio, TX Psychol. Corp.

Wihan, J., Grosch, J., Kalinichenko, L.S., Müller, C.P., Winkler, J., Kohl, Z., 2019. Layer-specific axonal degeneration of serotonergic fibers in the prefrontal cortex of aged A53T α-synuclein–expressing mice. Neurobiol. Aging. https://doi.org/10.1016/j.neurobiolaging.2019.03.014

Wilson, A.A., Ginovart, N., Hussey, D., Meyer, J., Houle, S., 2002. In vitro and in vivo characterisation of [11C]-DASB: A probe for in vivo measurements of the serotonin transporter by positron emission tomography. Nucl. Med. Biol. https://doi.org/10.1016/S0969-8051(02)00316-5

Table 1: Demographic Characteristics and Neuropsychological Results for the Late-Life Depressed (LLD) Patients and Controls

	Healthy, Older Controls (n = 20)	LLD Patients (n = 20) at Baseline (Prior to SSRI Treatment)	LLD Patients (n = 19) During SSRI Treatment
Age	66 ± 6	67 ± 6	
Sex (F/M)	11/10	11/10	
Education (in years)	15 ± 3	16 ± 2	
MMSE	29 ± 1	29 ± 1	29 ± 1
HAMD	1 ± 1	18 ± 2[a]	5 ± 3[c]*
BDI	6 ± 12	24 ± 8[b]	7 ± 2[d]*
CVLT Total Recall (Sum of first 5 Trials)	59 ± 12	57 ± 10	58 ± 10
CVLT Delayed Free Recall	12 ± 2	12 ± 3	13 ± 3
BVMT-R Total Recall (Sum of first 3 Trials)	19 ± 7	20 ± 8	24 ± 7[e]
BVMT-R Delayed Recall	8 ± 3	7 ± 3	9 ± 3[e]
Rey Complex Figure Test-Copy	32 ± 3	31 ± 4	32 ± 3
Rey Complex Figure Test-Immediate Recall	17 ± 6	15 ± 7	21 ± 7[f]
Rey Complex Figure Test-Delayed Recall	16 ± 5	14 ± 6	21 ± 7[g]
DKEFS™ Letter Fluency	44 ± 12	40 ± 12	46 ± 12
DKEFS™ Category Fluency	41 ± 8	42 ± 8	42 ± 8

23

BDI, Beck Depression Inventory; BVMT-R, Brief Visual Memory Test-Revised; CVLT, California Verbal Learning Test, D-KEFS™, Delis-Kaplan Executive Function System™; HAMD, Hamilton Depression Rating Scale; MMSE, modified Mini-Mental State Examination; SSRI, Selective Serotonin Reuptake Inhibitor.

*tests performed prior to the PET scan.

[a]Significant between group difference (F(1,18)=205.6, *P* = 0.000)
[b]Significant between group difference (F(1,18)=38.00, *P* = 0.000)
[c]Significant difference in the LLD patients before and during SSRI treatment (F(1,18)=229.31, *P* = 0.000)
[d]Significant difference in the LLD patients before and during SSRI treatment (F(1,18)=42.52, *P* = 0.000)
[e]Significant difference in the LLD patients before and during SSRI treatment (F(1,18)= 14.06, *P* = 0.001)
[f]Significant difference in the LLD patients before and during SSRI treatment (F(1,18)=33.80, *P* = 0.000)
[g]Significant difference in the LLD patients before and during SSRI treatment (F(1,18)= 61.10, *P* = 0.000)

Table 2: Serotonin Transporter Availability in Late-Life Depressed (LLD) Patients Scanned Prior to Starting Antidepressant Treatment Compared to Demographically-Matched Controls: Volume of Interest Analysis (VOI). Sample Size (Healthy Controls: n=20; LLD patients n=20).

	Healthy Controls	LLD Patients	F Ratio	*P* Value	Effect Size
BPnd for [11C]-DASB VOI's					
Cortical Regions					
Cingulate Gyrus	0.54 ± 0.16	0.51 ±0.12	0.39	0.537	-0.21
Frontal Cortex	0.33 ± 0.11	0.32 ±0.10	0.20	0.659	-0.10
Temporal Lobe	0.32 ± 0.08	0.27 ±0.09	3.24	0.080	-0.58
Pre-central Gyrus	0.30 ± 0.10	0.32 ±0.12	0.24	0.624	0.18
Post-Central Gyrus	0.33 ± 0.12	0.34 ±0.14	0.08	0.772	0.08
Parietal Lobe	0.29 ±0.09	0.31 ±0.11	0.62	0.435	0.19
Occipital Lobe	0.36 ±0.08	0.34 ±0.12	0.37	0.548	-0.20
Insula	0.76 ±0.17	0.70 ±0.14	1.76	0.193	-0.37
Sub-Cortical Regions					
Caudate	1.17 ±0.33	0.97 ±0.28	**4.16**	0.048	-0.63
Putamen	1.67 ±0.33	1.56 ±0.24	1.61	0.212	-0.38
Globus Pallidus	1.51 ±0.33	1.40 ±0.30	1.15	0.289	-0.35
Ventral Striatum	1.77 ±0.35	1.65 ±0.22	1.82	0.185	-0.40
Thalamus	1.46 ±0.28	1.39 ±0.26	0.61	0.439	-0.26
Brainstem	1.06 ±0.18	0.97 ±0.24	1.68	0.203	-0.42
Limbic Regions					
Amygdala	1.48 ±0.25	1.33 ± 0.28	3.38	0.074	-0.55
Hippocampus	0.52 ±0.13	0.43±0.12	**4.88**	0.033	-0.69
Entorhinal Cortex	0.56 ±0.13	0.39±0.15	**15.03**	0.000	-1.03
Parahippocampal Gyrus	0.46 ±0.12	0.36±0.12	**7.18**	0.011	-0.78

24

Table 3: Serotonin Transporter Availability in Late-Life Depressed (LLD) Patients Scanned Prior to Starting Antidepressant Treatment Compared to Demographically-Matched Controls: Volume of Interest Analysis (VOI) Sub-Divided into Braak Stages. Sample Size (n=20).

	Healthy Controls	LLD Patients	F Ratio	*P* Value
BPnd for [^{11}C]-DASB VOI's				
Braak I	0.56 ± 0.13	0.39 ± 0.15	15.03	0.001
Braak II	0.52 ± 0.13	0.43 ± 0.12	4.88	0.033
Braak III	0.47 ± 0.10	0.43 ± 0.12	1.894	0.177
Braak IV	0.60 ± 0.13	0.55 ± 0.12	1.61	0.212
Braak V	0.39 ± 0.11	0.38 ± 0.10	0.14	0.713
Braak VI	0.35 ± 0.11	0.36 ± 0.13	0.03	0.876

Table 4: Lower Serotonin Transporter Availability in Late-Life Depressed (LLD) Patients scanned prior to starting antidepressant treatment Compared to Demographically-Matched Controls: Voxel Wise Analysis. Sample Size (n=20).

Left Hemisphere				Right Hemisphere		
MNI[1] Coordinates	Talairach Coordinates	Z-Score		MNI Coordinates	Talairach Coordinates	Z-Score
X Y Z (mm)	X Y Z (mm)		Structure	X Y Z (mm)	X Y Z (mm)	
-18 -12 -20	-18 -8 -15	3.63	Lateral Orbital Gyrus (BA 11)			
			Insula	38 -2 -20		3.23
-48 -14 -24	-45 -14 -17	3.90	Superior Temporal Gyrus (BA 38)			
-44 -4 -14	-42 -7 -8	3.54	Superior Temporal Gyrus (BA 22)			
			Middle Temporal Gyrus (BA 20/21)	66 -16 -22	62 -19 -14	3.10
-44 -10 -34	-42 -13 -26	3.12	Inferior Temporal Gyrus (BA 20)	56 -12 -32	53 -15 -24	3.52
-28 -16 -28	-27 -14 -23	4.24	Parahippocampal	30 -12 34	27 -10 -27	4.40

25

			Gyrus (BA 36)			
-26 0 -30	-26 -3 -23	3.09	Parahippocampal Gyrus (BA 36)			
			Amygdala	30 -6 -14		3.50
-30 0 -42	-28 2 -34	3.89	Fusiform Gyrus (BA 37/20)	32 0 40	29 2 -31	4.25

Significant between-group comparisons are reported at a cluster-level, family-wise error (FWE) corrected threshold of p = 0.000 and a peak voxel uncorrected threshold of $p \leq 0.001$: Height threshold p=0.01 and extent threshold (k) =50 voxels. The cluster size (k_E) is 6875. BA, Brodmann area; MNI, Montreal Neurological Institute (MNI). Sample Size (n=20).

Table 5. Mean BP_{ND} values (± SD), estimates of O_{max} and IC_{50}, and mean occupancy values in 10 representative regions whose mean baseline BP_{ND} values exceeded 0.5.

	BP_{ND} of [^{11}C]DASB	O_{max} (%)	IC_{50} (ng/mL)	Mean occupancy
Caudal anterior cingulate	0.57 ± 0.15	85.1	8.25	74.2 ± 11.8
Rostral anterior cingulate	0.54 ± 0.13	83.3	3.77	78.1 ± 10.4
Insula	0.71 ± 0.16	85.8	3.48	80.7 ± 8.1
Posterior cingulate	0.58 ± 0.18	60.3	0.02	60.3 ± 12.7
Amygdala	1.38 ± 0.30	97.4	5.01	89.4 ± 7.0
Caudate nucleus	1.00 ± 0.27	95.7	2.94	90.9 ± 10.1
Putamen	1.58 ± 0.25	75.4	2.08	72.7 ± 5.8
Globus Pallidus	1.48 ± 0.32	76.7	4.29	71.2 ± 6.8
Ventral striatum	1.78 ± 0.29	87.8	3.17	83.0 ± 5.5
Thalamus	1.4 ± 0.27	81.9	3.61	76.9 ± 4.8

Binding potential, BP_{ND}; maximal attainable occupancy, O_{max}; Half maximal inhibitory concentration, IC50. Sample size (n=16) LLD patients treated with Citalopram

Table 6a: Correlation between 5-HTT Occupancy in Late-Life (LLD) Depressed Patients and the Change in Depressive Symptoms (Beck Depression Inventory)

Left Hemisphere				Right Hemisphere		
MNI Coordinates	Talairach Coordinates	Z-Score		MNI Coordinates	Talairach Coordinates	Z-Score
X Y Z (mm)	X Y Z (mm)		Structure	X Y Z (mm)	X Y Z (mm)	
-14 -30 44	-13 -28 41	3.20	Paracentral Lobule (BA 5)			
-8 -24 38	-7 -22 36	3.40	Posterior Cingulate Gyrus (BA 31)	0 -10 30	0 -9 29	3.57

Significant correlations are reported at a cluster-level, family-wise error (FWE) corrected threshold of p = 0.036 and a peak voxel uncorrected threshold of $p \leq 0.001$: Height threshold p=0.01 and extent threshold (k) =50 voxels. The cluster size (k_E) is 1509. BA, Brodmann area; MNI, Montreal Neurological Institute (MNI). Sample Size (n=19) LLD patients treated with Citalopram (n=16) and Sertraline (n=3) included.

Table 6b: Correlation between 5-HTT Occupancy in Late-Life Depressed (LLD) Patients and the Change in Visual-Spatial Memory (Brief Visual Memory Test-Revised)

Left Hemisphere				Right Hemisphere		
MNI Coordinates	Talairach Coordinates	Z-Score		MNI Coordinates	Talairach Coordinates	Z-Score
X Y Z (mm)	X Y Z (mm)		Structure	X Y Z (mm)	X Y Z (mm)	
-32 -10 14	-31 -11 15	3.52	Insula (BA 13)	38 -14 12	36 -14 14	3.63
-32 -22 8	-30 -22 10	3.36	Insula (BA 13)	42 6 -16	40 1 -9	3.09
-38 0 8	-36 -2 10	3.24	Insula (BA 13)			
			Superior Temporal Gyrus (BA 22)	46 -10 -8	43 -12 -2	3.67
			Middle Temporal	52 -16 -12	49 -18 -6	3.40

27

			Gyrus (BA 22)			
			Inferior Temporal Gyrus (BA 20)	56 -28 -26	53 -30 -18	4.07
-48 -26 10	-45 -26 12	3.08	Transverse Temporal Gyrus	42 -18 6	40 -19 9	3.85
-8 -58 10	-7 -56 12	3.39	Precuneus (BA23)	14 -52 24	14 -50 24	3.85
-2 -12 30	-1 -11 29	3.09	Posterior Cingulate (BA 23)	10 -24 36	10 -22 34	4.03
-34 -48 -16	-32 -49 -9	3.08	Fusiform Gyrus (BA 37)	48 -44 -16	46 -45 -9	3.41
-48 -26 10	-45 -26 12	3.08	Supramarginal Gyrus (BA 40)	56 -24 20	54 -23 21	3.73
			Supramarginal Gyrus (BA 40)	44 -24 16	42 -24 17	3.25
-2 -12 30		3.09	Posterior Cingulate			
			Pericalcarine Gyrus	24 -66 10	24 -64 12	3.71
			Pericalcarine Gyrus	22 -68 6	22 -66 9	3.68
			Pericalcarine Gyrus (BA 23)	18 -60 8	18 -58 11	3.24
			Isthmus/Cingulate (BA 18)	10 -42 4	10 -42 7	3.17
			Lingual Gyrus (BA 18)	14 -54 4	14 -53 7	3.14
-28 -20 -8	-27 -21 -3	3.34	Hippocampus			
-26 6 4		3.42	Putamen	28 4 6		3.91
			Putamen	30 -14 4		3.43
-26 -16 -4		3.31	Globus Pallidus	20 -6 6		3.08
-24 -10 8		3.22	Globus Pallidus			
-22 -24 12		3.83	Thalamus	22 -28 2		3.22
-14 -16 4		3.24	Thalamus			

28

Significant correlations are reported at a cluster-level, family-wise error (FWE) corrected threshold of $p = 0.000$ and a peak voxel uncorrected threshold of $p \leq 0.001$: Height threshold p=0.01 and extent threshold (k) =50 voxels. The cluster size (k_E) is 15029. BA, Brodmann area; MNI, Montreal Neurological Institute (MNI). Sample Size (n=19) LLD patients treated with Citalopram (n=16) and Sertraline (n=3) included.

Figure 1 Decreased Serotonin Transport Availability in Late-Life Depressed Patients and Healthy Controls. Voxel-wise Analysis of Parametric [^{11}C]-DASB Images. Statistically significant voxel-wise results are displayed on an MRI.
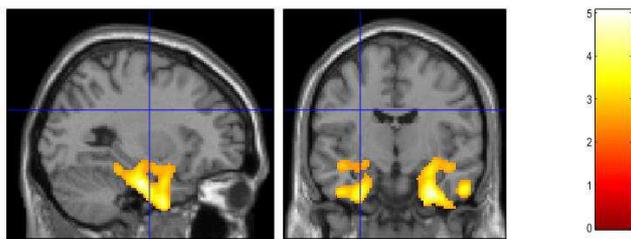

Figure 2 Serotonin Transporter Occupancy by Antidepressants in Late-Life Depressed Patients Voxel-wise Analysis of Parametric [^{11}C]-DASB Images. Statistically significant voxel-wise results are displayed on an MRI. (n = 16 Late-Life Depressed Patients treated with Citalopram and 3 with Sertraline).
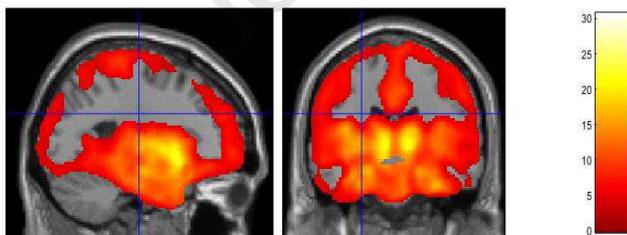
**Figure 3.** 5-HTT occupancy in the thalamus versus plasma Citalopram concentrations. The data fit best when O_{max} was estimated (dotted curve) than when O_{max} was fixed at 100% (dashed curve). N=16 LLD patients treated with Citalopram

29
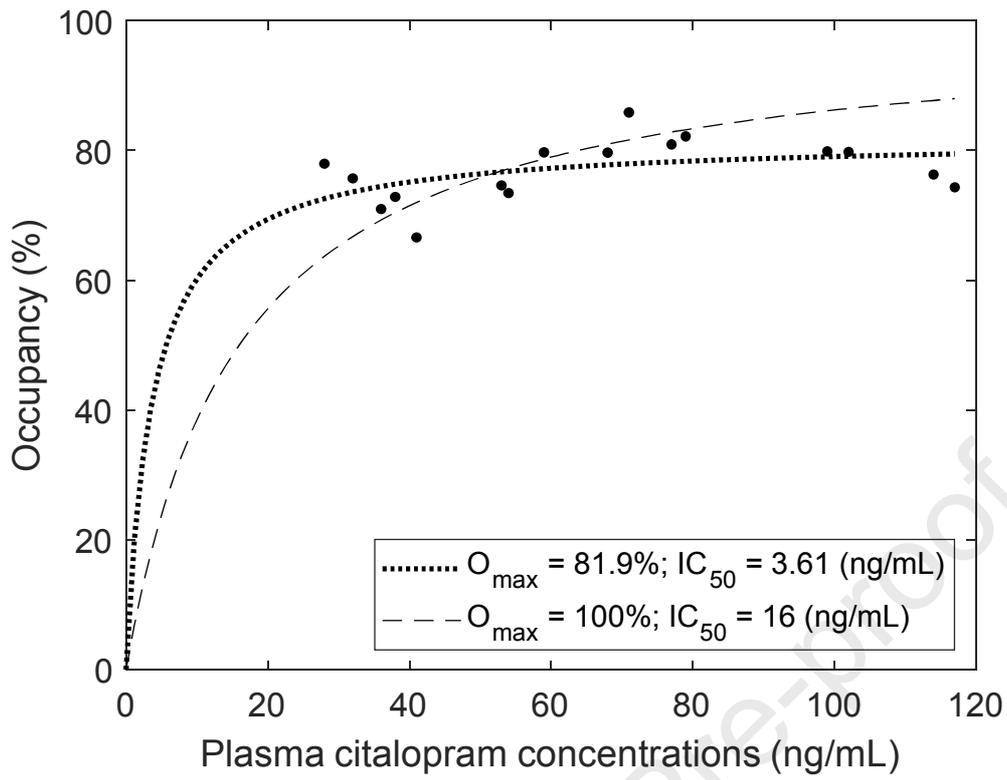
Supplemental Materials

Plasma Citalopram and Metabolites

Plasma Citalopram and two metabolites desmethyl- and didesmethylCitalopram were measured using a previously published liquid chromatographic method (Oyehaug, et.al., 1982). The procedure was modified slightly by using a more polar reversed-phase column (trimethylsilyl bonded silica) and altering the mobile phase to 72: 28 phosphate buffer:acetonitrile with the pH adjusted to 3.2 with phosphoric acid and n-butylamine with a flow rate at 1.5 ml/min. A fluorescence detector set at 235nm $_{excit.}$ and 300nm $_{emiss.}$ produced clean chromatograms with no interference from other drugs or endogenous material. The method was validated from 300 ng/ml to the lower limit of quantitation (2.5 ng/ml) resulting in an intra-day variation of no more than 10% for all 3 compounds at 7 concentrations of the calibration curve. Inter-day variation did not exceed 6.8% for the 3 quality controls over 16 consecutive days.

Plasma Sertraline and DesmethylSertraline

Plasma Sertraline and its main metabolite desmethylSertraline are quantitated using liquid chromatography with fluorescence detection following pre-column derivatization with dansyl chloride. The method is based upon a previously published procedure for fluoxetine and norfluoxetine with some minor modifications (Suckow et al., 1992). In short, one ml of plasma sample containing 150 ng of the bromo analog of Sertraline as the internal standard is rendered alkaline with carbonate buffer and extracted with 6 ml of 20% ethyl acetate in *n*-heptane. After mixing and centrifuging, the organic phase is back-extracted with 150 μl of dilute HCl. Following mixing and centrifuging, the organic phase is aspirated and discarded, and the aqueous phase evaporated to dryness. The residue is derivatized with 1% dansyl chloride for 45 minutes at room temperature, evaporated to dryness and reconstituted with mobile phase. Chromatography is carried out using a Supelco LC-18 (250 x 4.6 mm, 5μ) column and a mobile phase of 17:10:73 phosphate buffer: methanol: acetonitrile at a flow rate of 2.0 ml/min. The eluent is monitored using a fluorescence detector with the excitation and emission wavelengths set at 255 nm and 515 nm, respectively. The calibration curve is linear between 800 and 10 ng/ml and the minimum quantifiable level is about 5 ng/ml. Total chromatographic analysis time is less than 15 minutes with an intra-day imprecision error not exceeding 4.3% and 3.8% for Sertraline and desmethylSertraline, respectively (n = 12 for each calibration concentration). Inter-day imprecision based upon the three levels of quality controls that are included with each run did not exceed 4.3 % for Sertraline and 8.9% for desmethylSertraline (n = 10 days).

31

Oyehaug E, Ostensen ET, Salvesen B, Determination of the antidepressant agent Citalopram and metabolites in plasma by liquid chromatography with fluorescence detection, *J. Chromatogr., 227,* 129-135(1982).

Suckow RF, Zhang MF, Cooper TB, Sensitive and selective liquid chromatographic assay of fluoxetine and norfluoxetine in plasma with fluorescence detection after pre-column derivatization, *Clin. Chem., 38,* 1756-1761(1992).

Supplemental Table 1: Serotonin Transporter Occupancy by Antidepressant Treatment in Late-Life Depressed (LLD) Patients

Left Hemisphere				Right Hemisphere		
MNI Coordinates	Talairach Coordinates	Z-Score		MNI Coordinates	Talairach Coordinates	Z-Score
X Y Z (mm)	X Y Z (mm)		Structure	X Y Z (mm)	X Y Z (mm)	
0 -46 32	0 -44 -31	6.12	Isthmus/ Cingulate (BA 23)	2 -32 34	2 -30 32	6.34
-4 -2 44	-3 0 40	6.97	Cingulate Gyrus (BA 24)	4 -6 42	4 -4 39	6.84
-2 36 18	-2 34 17	7.77	Rostral Anterior Cingulate (BA 32)	0 42 8	0 38 7	7.21
-4 22 -10	-4 18 -7	7.59	Rostral Anterior Cingulate (BA 32/BA 11)	2 24 -10	1 20 -7	7.36
-2 36 -10	-2 31 -9	7.02	Rostral Anterior Cingulate (BA 32)			
-2 12 38		7.21	Caudal Anterior Cingulate (BA 32)			
-14 62 14	-14 58 11	5.40	Superior Frontal Gyrus (BA 10)	18 64 -10	17 58 -10	5.32

-2 28 -20	-2 23 -17	7.42	Medial Orbital Gyrus (BA 11)			
-2 58 -2	-2 52 -4	6.47	Medial Orbital Gyrus (BA 10)			
-24 40 -16	-24 35 -14	5.65	Lateral Orbital Gyrus (BA 11)	14 16 -16	13 12 -11	7.78
-40 -14 12	-38 -15 13	7.09	Insula (BA 13)	40 -6 4	38 -8 0	7.57
			Insula (BA 13)	40 -6 -4	38 -8 6	7.57
			Insula (BA 13)	38 6 -14	36 2 -8	7.31
			Insula (BA 13)	36 20 -2	34 17 2	6.81
-40 20 -28	-39 14 -22	6.77	Superior Temporal Gyrus (BA 38)	44 18 -26	42 12 -18	6.46
			Anterior Temporal Lobe (BA 38)	36 14 -30	35 8 -22	6.65
			Middle Temporal Gyrus (BA 20)	46 10 -36	44 4 -27	5.75
			Inferior Temporal Gyrus (BA 38)	32 8 -44	31 2 -35	5.79
-28 -18 -28	-27 -20 -20	6.66	Parahippocampal Gyrus (BA 36)	28 -4 -34	27 -7 -25	7.16
-20 2 34	-20 -2 -26	6.64	Parahippocampal Gyrus (BA 36)			
-20 -2 -24		6.75	Amygdala	24 -4 -20		7.44
-20 -24 -18		7.31	Hippocampus	24 -12 -18		7.48
-20 -14 -18		7.31	Hippocampus			
-34 -18 -22	-32 -20 -15	6.61	Hippocampus			
-34 -26 64	-34 -22 58	5.68	Post-Central Gyrus (BA 1)	22 -34 74	23 -29 66	6.30
-20 -58 8	-19 -57 11	6.42	Precuneus (BA 23)	20 -56 6	20 55 9	5.82
-44 -44 -26	-42 -40 -24	5.47	Fusiform Gyrus (BA 37)	24 -36 -20	21 -34 -17	6.31
-52 -28 12	-49 -28 14	6.01	Supramarginal			

33

			Gyrus (BA 41)			
			Pericalcarine Gyrus (BA 17)	12 -64 -12	12 -62 14	5.87
			Pericalcarine Gyrus (BA 23)	22 -66 8	22 -64 11	5.76
			Lingual Gyrus (BA 18)	20 -48 0	20 -47 4	6.11
-2 -66 12	-1 -64 14	6.09	Cuneus (BA 18)			
-8 -72 22	7 -69 22	5.48	Cuneus (BA 18)	14 -60 14	14 -58 16	5.87
-12 -2 12	-11 -3 13	6.62	Caudate			
-18 10 -10		Inf	Putamen	22 14 -6		7.83
-34 -6 -2		7.73	Putamen			
-26 -12 -8		7.72	Putamen			
-10 12 -8		Inf	Ventral Striatum	10 10 -6		7.83
-8 22 0		7.75	Thalamus	16 -26 4		Inf

Significant within-subject comparisons are reported at a cluster-level, family-wise error (FWE) corrected threshold of p = 0.000 and a peak voxel corrected threshold of $p \leq$ 0.001: Height threshold p=0.001 and extent threshold (k) =50 voxels. The cluster size (k_E) is 123749. Given the great number of significant peak voxels, the voxels within each brain region are reported with the highest z score that could be localized to a Talairach coordinate according to the atlas of Lacadie et al., (2008). BA, Brodmann area; MNI, Montreal Neurological Institute (MNI). Sample Size (n=19) LLD patients treated with Citalopram (n=16) and Sertraline (n=3) included.

Supplemental Figure 1

Correlation between Serotonin Transporter Occupancy in the Left Posterior Cingulate Gyrus And Change in Beck Depression Inventory Score in LLD patients treated with SSRI's (Sample Size n=16 LLD patents treated with Citalopram and n=3 LLD patients treated with Sertraline)

Change in Beck Depression Inventory Score

$r^2 = 0.498$ P < 0.05

Serotonin Transporter Occupancy in the Left Posterior Cingulate Gyrus

35
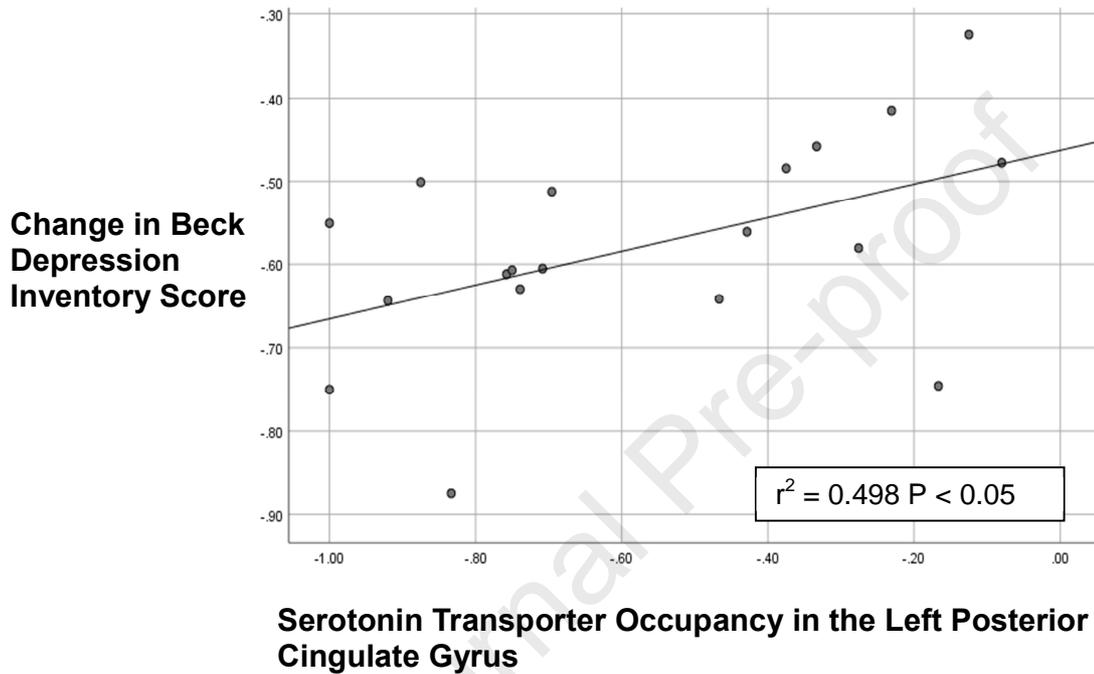
LLD patients show lower temporal cortical serotonin transporter binding than controls

5-HTT occupancy by antidepressant treatment is observed in cortical and limbic regions

5-HTT occupancy is correlated with improvement in visual-spatial memory